



Magnetic measurements and geochemical characterization of the road-deposited sediments (RDS), Allahabad city, India: impact of climatic perturbations on sediment composition and provenance tracing

Ambalika Niyogi¹ · Jayanta Kumar Pati^{1,2} · Shiva Kumar Patil³ · Dipak Panda⁴ · Munmun Chakarvorty¹

Received: 27 February 2017 / Accepted: 28 January 2018 / Published online: 8 March 2018
© Springer-Verlag GmbH Germany, part of Springer Nature 2018

Abstract

Purpose Magnetic measurements provide quantitative data on urban pollution (including heavy metal content) which correlate significantly with geochemical analysis and better constrain the source character of pollutants. The present study is aimed to map the distribution of heavy metals in road-deposited sediments (RDS) and identify the possible provenance of the sediments during the pre-monsoon and post-monsoon (mainly fog) periods of Allahabad city, India.

Materials and methods In all, 442 RDS samples from 60 representative locations were collected over 3 years, and the different magnetic parameters and metal concentrations were determined. The magnetic minerals were identified using X-ray diffraction (XRD) and backscatter electron-scanning electron microscopy (BSE-SEM) while principal component analysis (PCA) was used for the provenance tracing of the RDS.

Results and discussion The samples record high magnetic susceptibility (χ_{lf} ; \bar{x} : $174.44\text{--}604.36 \times 10^{-8} \text{ m}^3 \text{ kg}^{-1}$), saturation isothermal remnant magnetization (SIRM; \bar{x} : $1586.30\text{--}2421.51 \times 10^{-5} \text{ A m}^2 \text{ kg}^{-1}$) and anhysteretic remnant magnetization susceptibility (χ_{ARM} ; \bar{x} : $461.64\text{--}1099.68 \times 10^{-8} \text{ m}^3 \text{ kg}^{-1}$) values independent of seasonal change. The magnetic minerals in the sediments lie in pseudo-single domain (PSD) and multi-domain (MD) from anthropogenic sources while stable single domain (SSD) is associated with both natural and anthropogenic sources. PCA of magnetic proxies with heavy metal concentrations suggests the derivation of the RDS from multiple (crustal, anthropogenic, traffic, and industrial) sources. The XRD analyses confirm the presence of magnetite and hematite, in addition to quartz, feldspar, gypsum, apatite, calcite, and dolomite in the RDS. Limited geochemical analysis of the RDS comprising Na, Mg, Al, K, Ca, Ti, Mn, Fe, Sc, V, Cr, Ni, and Rb suggests a predominance of anthropogenic load in RDS compared to geogenic sources.

Conclusions The magnetic measurements coupled with XRD and BSE-SEM analyses suggest the dominance of magnetic grains and heavy metals in pre-monsoon samples compared to those collected during the fog period. The geochemical data also support the seasonal control for the elevated heavy metal concentration in the RDS and their derivation from geogenic as well as anthropogenic sources.

Keywords Heavy metal · Magnetic measurements · Pre-monsoon · Provenance · Road-deposited sediments · Urban pollution

Responsible editor: Ian Foster

✉ Ambalika Niyogi
ambalika.niyogi@gmail.com

³ Dr. K.S. Krishnan Geomagnetic Research Laboratory, Leelapur Road, Hanumanganj, Allahabad 221505, India

¹ Department of Earth and Planetary Sciences, Nehru Science Centre, University of Allahabad, Allahabad 211002, India

² National Centre of Experimental Mineralogy and Petrology, 14 Chatham Lines, University of Allahabad, Allahabad 211002, India

⁴ EPMA Laboratory (PLANEX), Physical Research Laboratory, Thalje Campus, Ahmedabad 380009, India

1 Introduction

Magnetic measurements are rapid, cost-effective, require less time for sample preparation, are non-destructive (Dekkers 1997; Evans and Hellers 2003; Maher 2011), and are widely applied to decode the distribution of heavy metal contaminants and trace their sources (Robertson et al. 2003; Lu et al. 2007; Karimi et al. 2011). The analyses of various magnetic parameters (χ_{lf} , $\chi_{fd}\%$, χ_{ARM} , SIRM, and S-ratio%) are extensively employed to estimate anthropogenic pollution (Adachi and Tainosho 2005; Qiao et al. 2011; Fedotov et al. 2014; Szuszkiewicz et al. 2015; Zhang et al. 2015; Wang 2016). The cosmopolitan centers of the world, like Delhi, India (Meena et al. 2011), Beijing, China (Li et al. 2014), and Manchester, United Kingdom (Jones et al. 2015), are pervasively affected with magnetic particulate matter derived from multiple sources. The application of magnetic proxies to monitor urban (Qiao et al. 2011; Jordanova et al. 2015), industrial (Wang and Qin 2005), and agricultural (Bian et al. 2014) pollution is well known. In recent years, the magnetic measurements of the RDS are coupled with their geochemical analyses to better relate the source to sink (Jordanova et al. 2015; Bourliva et al. 2016). The dust load from multiple sources is best concentrated and homogenized in and around the city road networks making them ideal sites for representative sampling. In India, some of the densely populated, industrialized, highly polluted urban centers are located in the north (New Delhi, Pant et al. 2015; Agra, Pipal et al. 2011; Kanpur, Rai et al. 2016; Allahabad, Chakarvorty et al. 2014; and Varanasi, Pandey et al. 2017), and these centers experience severe winter fog every year. According to a recent report, one of these cities, Allahabad, is the third most polluted in the world (WHO Global Urban Ambient Air Pollution Database 2016). In addition to its large permanent population, the Allahabad city experiences a sudden increase of inhabitants (~120 million) for a religious festival (December–February; “Magh Mela”) leading to a spurt in the anthropogenic movement. Hence, the impact of heightened anthropogenic activity and seasonal change can be better understood by a multi-parameter study of the RDS involving magnetic measurements and geochemical analysis in the present study.

2 Materials and methods

2.1 Study area

The city of Allahabad (25°27'33.40"-25°26'33.40"N and 81°52'45.47"-81°52'33.40"E) is over 70 km² in area and located in the northern Indian state of Uttar Pradesh. It is one of the oldest cities of India and is a famous pilgrimage center with a population of 5,954,391 inhabitants (2011 Census) and having a population density of 1086 people per km².

The annual mean temperature is 26.1 °C and average precipitation of ~1027 mm. The wind direction is mostly north-westerly. The city has a humid subtropical climate with three major seasons: hot dry summer (April–July), warm humid monsoon (August–October), and cool dry winter (November–March). The topography of the city is nearly flat with average elevation of 98 m and is located within the Indo-Gangetic Basin. The city is situated at the confluence of two major Himalayan Rivers, the Ganga and Yamuna.

2.2 Sampling zones

The sampling locations were divided into five zones based on urban characteristics; these were green area, commercial area, residential area, traffic area, and industrial area. The zone 1 (Cantonment: N 25°27'30.20" E 81°48'57.41") is a green area comprising trees and grasses with a group of residential colonies, where the entries of heavy vehicles are restricted and the use of polythene is banned. The zone 2 (Civil Lines: N 25°27'1.16" E 81°50'3.86") is known for major commercial activity. The zone 3 (Chawk: N 25°26'17.63" E 81°50'1.06") is a commercial and residential area having moderate to high traffic density. The zone 4 (Alopibagh: N 25°26'34.42" E 81°52'8.65") is in the vicinity of National Highway (NH-2) having high traffic density. In addition, the area comprises residential as well as commercial establishments. The zone 5 contains the industrial areas Naini (N 25°23'13.70" E 81°51'59.24") and Phulpur (N 25°32'1.80" E 82°3'58.38"). The former area has many industries such as manufacturing units, electrical units, warehouses etc. located toward south while the latter location is situated at the north-eastern part of the city and is known for the coal-fired power plant (Indian Farmers Fertilizers Cooperative; IFFCO) (Fig. 1).

2.3 Sampling and laboratory procedures

In order to investigate the spatio-temporal distribution pattern of magnetic particles causing urban pollution, the magnetic susceptibility of 442 RDS samples collected during the present study (Fig. 1) from three sampling periods (pre-monsoon-2009: 1st April to 31st May, 2009; fog-2010: 1st–31st January and 1st–31st December, 2010; fog-2011: 1st–31st January and 1st–31st December, 2011) were measured. Thereafter, only 60 representative samples (20 samples from each of the three sampling periods) were selected from five representative zones spread over three seasons for detailed magnetic measurements (such as SIRM, χ_{ARM} , $\chi_{ARM}/SIRM$, SIRM/ χ_{lf} , χ_{ARM}/χ_{lf} , SOFT, S-ratio%), microscopic and chemical studies. The samples were collected with the help of brush and dust pan and were transferred to plastic bottles of 200 g capacity. The samples were air-dried, and then sieved using brass sieve of 35 ASTM (American Society for Testing and Materials, USA) mesh (500 μ m) to remove coarse debris and

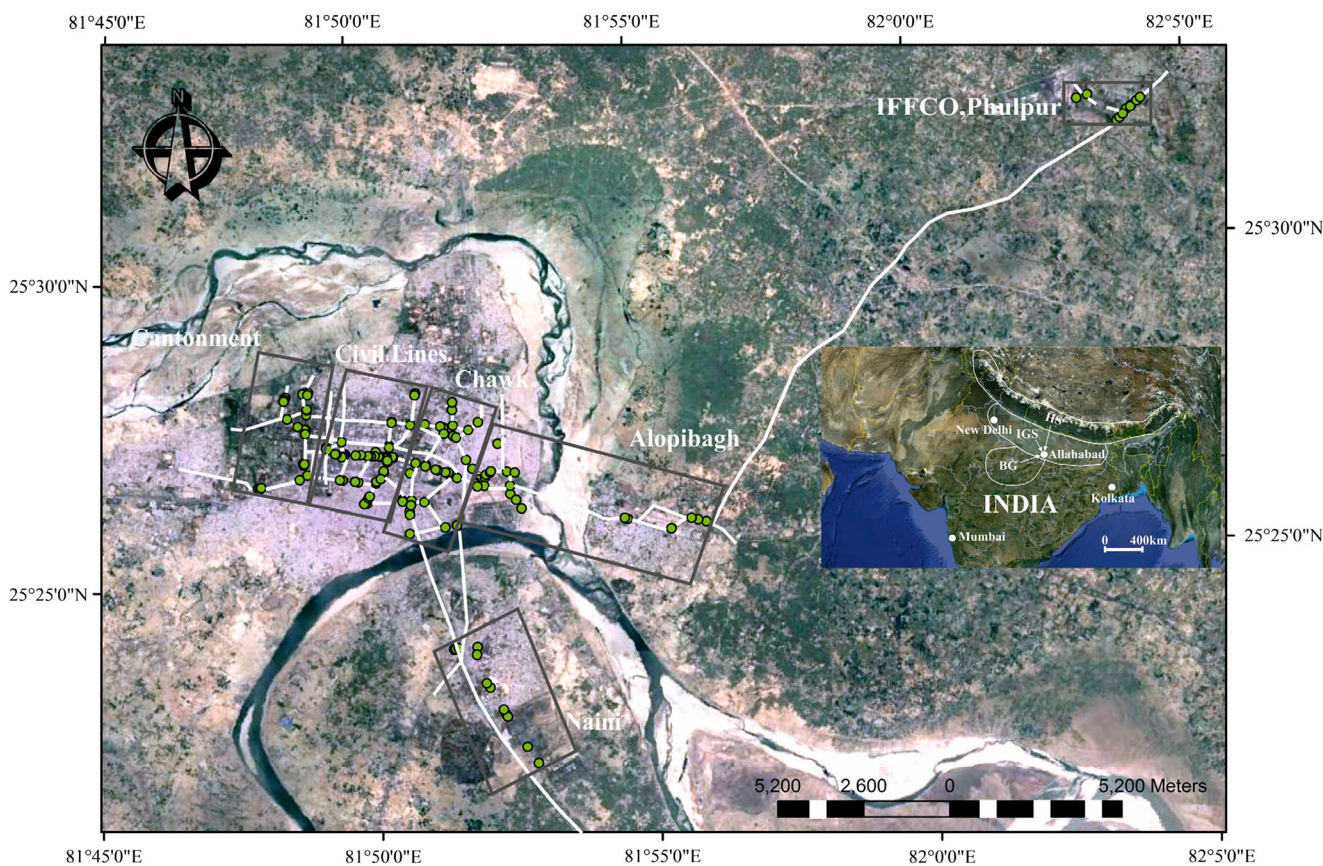


Fig. 1 The Google Earth® image of the study area showing sampling zones and individual locations and the possible provenance (HS, IGS, and BG) of sediments are given in the inset map

stones (Niyogi et al. 2011). The XRD was performed on the powdered samples (~ 200 mesh size/ $74 \mu\text{m}$) with accelerating voltage of 30 kV and beam current of 25 mA using $\text{CuK}\alpha$ target and Ni filter. The analytical conditions for all sample scans made between 10 and 60° (2θ) at a scan speed of 2° per minute. The BSE-SEM analyses were performed using Cameca SX-100 Electron Probe Microanalyzer (EPMA) instrument, Physical Research Laboratory, Ahmedabad for the morphological and micro-chemical analyses. The samples were mounted on glass slides using synthetic glue (Araldite®) for the BSE-SEM analysis and coated with carbon.

The low (χ_{lf}) and high (χ_{hf}) frequency magnetic susceptibility measurements of RDS were performed on the $< 500 \mu\text{m}$ fraction using a dual frequency sensor (0.47 and 4.7 kHz) magnetic susceptibility meter (MS2B; Bartington, UK; Department of Earth and Planetary Sciences, University of Allahabad), and the values are reported in SI unit ($10^{-8} \text{ m}^3 \text{ kg}^{-1}$). The frequency-dependent magnetic susceptibility ($\chi_{fd}\% = \chi_{lf}\chi_{hf}/\chi_{lf}^*100\%$) was also calculated. χ_{ARM} ($10^{-8} \text{ m}^3 \text{ kg}^{-1}$) was measured in Molspin spinner magnetometer. Isothermal remanent magnetization ($\text{IRM} \times 10^{-5} \text{ A m}^2 \text{ kg}^{-1}$) was measured using Pulse magnetizer (Model-MMPM 10) in field of 20, 100, 300 mT and 1 T,

and again re-introduced for demagnetization in $-20, -30, -40, -50, -100,$ and -300 mT. The other magnetic parameters measured and calculated include SIRM ($10^{-5} \text{ A m}^2 \text{ kg}^{-1}$) that was measured at 1 T, χ_{ARM}/SIRM (10^3 m A^{-1}), SIRM/χ_{lf} (10^3 m A^{-1}), χ_{ARM}/χ_{lf} , SIRM/ARM , SOFT ($[\text{SIRM}-\text{IRM}_{20 \text{ mT}}]/2$)/mass $\times 10^{-5} \text{ A m}^2 \text{ kg}^{-1}$ (Wang et al. 2008), and S-ratio % ($\text{IRM}_{300 \text{ mT}}/\text{SIRM}$).

2.4 Geochemical analysis

Geochemical analysis was carried out to determine the relationship between metal pollution and magnetic properties of RDS. The geochemical analysis of limited major and trace elements (including heavy metals) was performed using X-ray fluorescence (XRF) (Philips PW1400 XRF Spectrometer, Physical Research Laboratory, Ahmedabad) and the calibration was made with GSD-9 and SDO-1 internal standards. The data is reported with 10% precision for all the analyses. The samples were first sieved using a 35 mesh/ $500 \mu\text{m}$ sieve to remove the larger particles, and for chemical analysis, the ~ 200 ASTM mesh/ $74 \mu\text{m}$ fraction was taken. The sample was then powdered using a planetary ball (agate) mill for homogenization. Approximately 2–3 g of sample was taken with wax as a binder for making pressed

pellets. Then, the concentration of major (Na, Mg, Al, K, Ca, Ti, Mn, and Fe) and trace elements (Sc, V, Cr, Ni, Rb, and Y) was measured and reported in weight % or ppm.

2.5 Statistical analysis

Statistical analysis was undertaken on large dataset to infer about the source provenance of the pollutants using SPSS 20 version (SPSS Inc., USA). The most common multivariate analysis method, PCA, was applied to the dataset for identifying relationships between magnetic and geochemical data and provenance identification. In the PCA, Varimax with Kaiser normalization was used as a rotation method in the analysis.

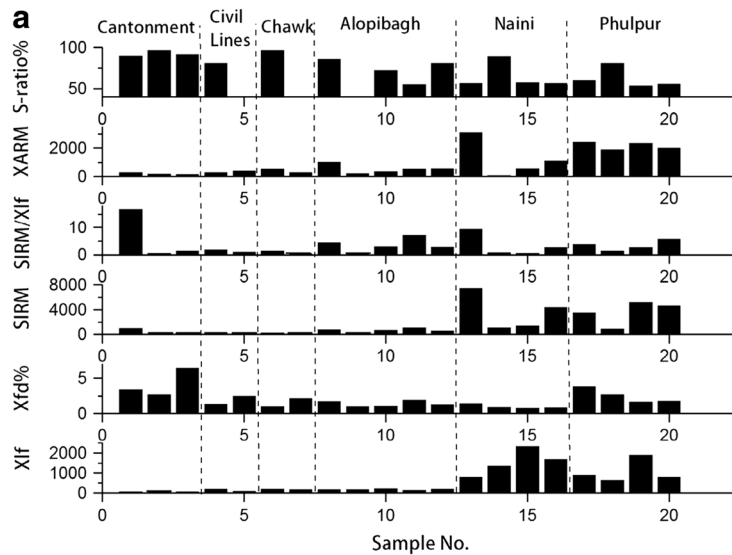
3 Results and discussion

3.1 Temporal and spatial variations of magnetic parameters of RDS within the city

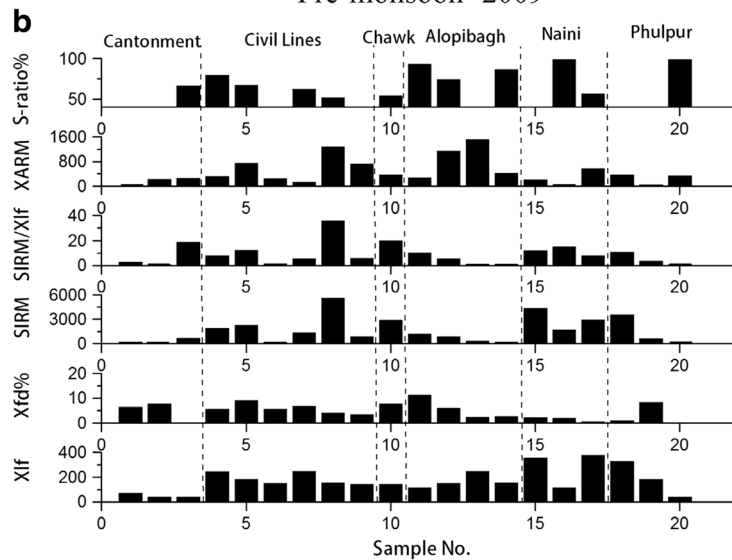
The results of magnetic measurements (χ_{lf} , $\chi_{fd}\%$, SIRM, SIRM/ χ_{lf} , χ_{ARM} , and S-ratio %) with reference to sampling time and zones are summarized in Fig. 2a–c and Table 1. The mean χ_{lf} of the RDS from the green area (zone 1) varies from 39.46 to $57.41 \times 10^{-8} \text{ m}^3 \text{ kg}^{-1}$ in pre-monsoon-2009. According to Canbay et al. (2010), the susceptibility value of the green area ranged from 10 to $21 \times 10^{-8} \text{ m}^3 \text{ kg}^{-1}$ while Lu et al. (2007) stated that the values ranged from 31 to $186 \times 10^{-8} \text{ m}^3 \text{ kg}^{-1}$ depending upon parent material, climate, geomorphology, vegetation, and time. The commercial area (zone 2, present study) shows wide variation in magnetic susceptibility ($81.5\text{--}187.26 \times 10^{-8} \text{ m}^3 \text{ kg}^{-1}$). The congested old city area falling in zone 3 shows limited variations (166.36 to $180.8 \times 10^{-8} \text{ m}^3 \text{ kg}^{-1}$). The susceptibility value in zone 4 is observed between 145.78 and $218.76 \times 10^{-8} \text{ m}^3 \text{ kg}^{-1}$. In contrast to the present study, the χ_{lf} of the residential and commercial areas of Turkey (Canbay et al. 2010) and China (Lu et al. 2007) ranged from 45 to 91 and 106 to $288 \times 10^{-8} \text{ m}^3 \text{ kg}^{-1}$, respectively, due to traffic emissions. The zone 5 comprising industrial areas of Naini and Phulpur record elevated values in the range of $799.78\text{--}2302.96 \times 10^{-8} \text{ m}^3 \text{ kg}^{-1}$ and $639.21\text{--}1916.14 \times 10^{-8} \text{ m}^3 \text{ kg}^{-1}$, respectively, whereas in China (Lu et al. 2007), it ranged from 111 to $1128 \times 10^{-8} \text{ m}^3 \text{ kg}^{-1}$ and 78 to $203 \times 10^{-8} \text{ m}^3 \text{ kg}^{-1}$ in Turkey (Canbay et al. 2010), respectively. It is interesting to note that these values are lower than those found in the present study. This could be due to relatively high industrial activities and traffic emissions in two select domains (Naini and Phulpur) of the study area. The $\chi_{fd}\%$ value during pre-monsoon-2009 lies between 0.76 and 6.45 with an average $\chi_{fd}\%$ of 2.02 suggesting the dominance of PSD, MD, and SSD grains compared

to fine superparamagnetic (SP) particles. The SIRM values of the RDS ranged from 27.4 to $7452.63 \times 10^{-5} \text{ A m}^2 \text{ kg}^{-1}$ (average, \bar{x} : 1677.73; standard deviation, σ : 2143.34) depicting significant variation. In samples belonging to pre-monsoon-2009, the χ_{ARM}/SIRM and χ_{ARM}/χ_{lf} values range between $0.05\text{--}7.16 \times 10^{-3} \text{ m A}^{-1}$ (\bar{x} : 1.73; σ : 1.99) and $0.04\text{--}6.35$ (\bar{x} : 2.68; σ : 1.7) suggesting a relatively high concentration of SSD magnetic minerals. The S-ratio % indicates the presence of low and high-coercivity magnetic minerals (magnetite and hematite) in the RDS with the variation of 53.28 to 96.67 (\bar{x} : 74.16; σ : 16.27) in pre-monsoon-2009. During the fog-2010, the magnetic susceptibility values vary from 37.87 to $379.2 \times 10^{-8} \text{ m}^3 \text{ kg}^{-1}$ (\bar{x} : 174.44; σ : 100.3) having high $\chi_{fd}\%$ value (0.66–11.26, \bar{x} : 5.15; σ : 3). The SIRM ranges from 19.09 to $5648.54 \times 10^{-5} \text{ A m}^2 \text{ kg}^{-1}$ (\bar{x} : $1586.3 \times 10^{-5} \text{ A m}^2 \text{ kg}^{-1}$; σ : 1572.32) while χ_{ARM}/SIRM and χ_{ARM}/χ_{lf} vary between $0.01\text{--}18.05 \times 10^{-3} \text{ m A}^{-1}$ (\bar{x} : 1.94; σ : 4.31) and 0.21–8.91 (\bar{x} : 3.38; σ : 2.93), respectively. The S-ratio % value ranges from 51.88 to 99.16 (\bar{x} : 74.27; σ : 17.18) during fog-2010. The χ_{lf} during fog-2011 varies from 29.42 to $1415.88 \times 10^{-8} \text{ m}^3 \text{ kg}^{-1}$ (\bar{x} : 297.59; σ : 326.27), the $\chi_{fd}\%$ ranges between 0.37 and 11.65 (\bar{x} : 4.66; σ : 3.28), and SIRM from 208.7 to $5266.38 \times 10^{-5} \text{ A m}^2 \text{ kg}^{-1}$ (\bar{x} : 2421.51; σ : 1448.1). The χ_{ARM}/SIRM ratio ranges from 0.07 to $6.71 \times 10^{-3} \text{ m A}^{-1}$ (\bar{x} : 0.77; σ : 1.48) and the χ_{ARM}/χ_{lf} lies from 1.14 to 27.27 (\bar{x} : 5.87; σ : 7.7). The S-ratio % value observed during fog-2011 lies from 65.12 to 94.74 (\bar{x} : 81.3; σ : 9.14) suggesting the presence of both low and high coercivity minerals.

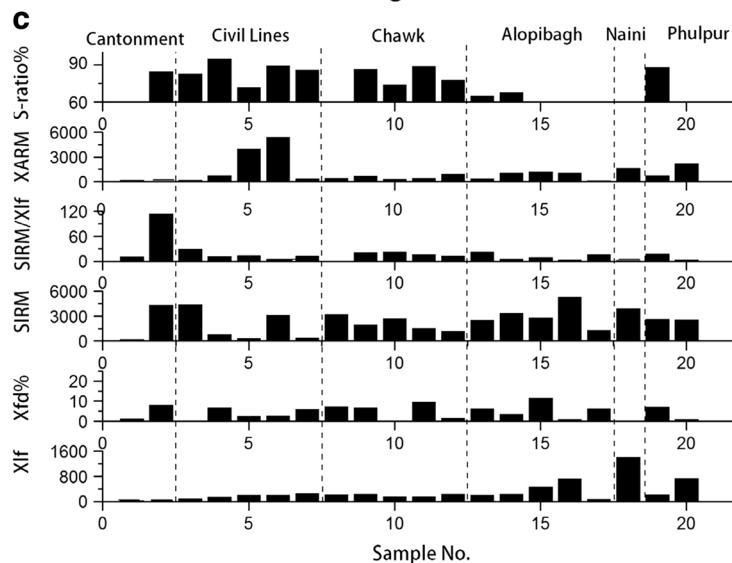
The present study dealing with the seasonal effects on the RDS reveals that unlike the fog period, the χ_{lf} values increase during pre-monsoon-2009 indicating a higher concentration of magnetic minerals. The $\chi_{fd}\%$ ranges between 0.37 and 11.65 during different seasons indicating the presence of MD and PSD grains with few SP particles. However, in zone 5, the $\chi_{fd}\%$ value is $< 3\%$ suggesting the possible contamination of RDS due to industrial activities. Thus, the increase in χ_{lf} decreases $\chi_{fd}\%$ and creates a threshold between low and high polluted zones. The χ_{ARM}/SIRM and χ_{ARM}/χ_{lf} values observed during the fog-2010 and 2011 were comparatively higher than pre-monsoon-2009 suggesting the presence of MD or PSD and coarse SSD grains. The King plot (King et al. 1982; Fig. 3a) and Dearing plot (Dearing 1999; Fig. 3b) show the presence of PSD and MD with coarse SSD but having low concentration of SP particles ($< 50\%$). The PSD and MD grains are generally derived from industrial activity, fuel combustion, and traffic pollution (Goddu et al. 2004; Sagnotti et al. 2006; Yang et al. 2010). The $\chi_{ARM}/\text{SIRM}\text{--}\chi_{ARM}/\chi_{lf}$ plot (Fig. 3c) shows the variation among SD ferrimagnetic grains having varied particle size similar to previous findings (Maher 1998). The higher value of χ_{ARM}/SIRM (1.9) indicates the presence of finer ($< 1 \mu\text{m}$) ferrimagnetic grains whereas the lower value



Pre-monsoon- 2009



Fog- 2010



Fog- 2011

◀ **Fig. 2 a–c** Data of various magnetic parameters obtained from the RDS collected from different zones of the study area between 2009 and 2011

points to the coarser fraction ($> 10 \mu\text{m}$) (Jones et al. 2015). In the present study, the finer ferrimagnetic grains show dominance in pre-monsoon-2009, whereas the coarse grains are

Table 1 Magnetic parameters measurement of RDS, Allahabad city, India

Sampling period	χ_{LF} ($10^{-8} \text{ m}^3 \text{ kg}^{-1}$)	$\chi_{\text{FD}}\%$	SIRM ($10^{-5} \text{ A m}^2 \text{ kg}^{-1}$)	χ_{ARM} ($10^{-8} \text{ m}^3 \text{ kg}^{-1}$)	$\chi_{\text{ARM}}/\text{SIRM}$ (10^{-3} m A^{-1})	SIRM/ χ_{LF} (10^{-3} m A^{-1})	$\chi_{\text{ARM}}/\chi_{\text{LF}}$	S-ratio%	SOFT ($10^{-5} \text{ A m}^2 \text{ kg}^{-1}$)
Pre-monsoon-2009	Max.	2302.96	6.45	7452.63	3116.14	7.16	16.71	6.35	96.67
	3-3-8-1-51								
	Min.	39.46	0.76	27.4	64.06	0.05	0.25	0.04	53.28
	Avg.	604.36	2.02	1677.73	920.73	1.73	3.42	2.86	74.16
σ	1.35	2143.34	921.74	1.99	3.95	1.7	16.27	867.34	
Fog-2010	6-9-4-68								
	Max.	379.2	11.26	5648.54	1523.77	18.05	36.31	8.91	99.16
	1-4-0-4-49								
	Min.	37.87	0.66	19.09	15.38	0.01	0.49	0.21	51.88
σ	3	1572.32	420.12	4.31	8.73	2.93	17.18	505.62	
Fog-2011	1-0-0-3								
	Max.	1415.88	11.65	5266.38	5400.28	6.71	113.88	27.27	94.74
	1-2-43								
	Min.	29.42	0.37	208.7	80.45	0.07	0.98	1.14	65.12
σ	3.28	1448.1	1363.53	1.48	24.03	7.7	9.14	416.44	
	3-2-6-27								
	Avg.	298.9	4.66	2421.51	1099.68	0.77	17.54	5.87	576.36

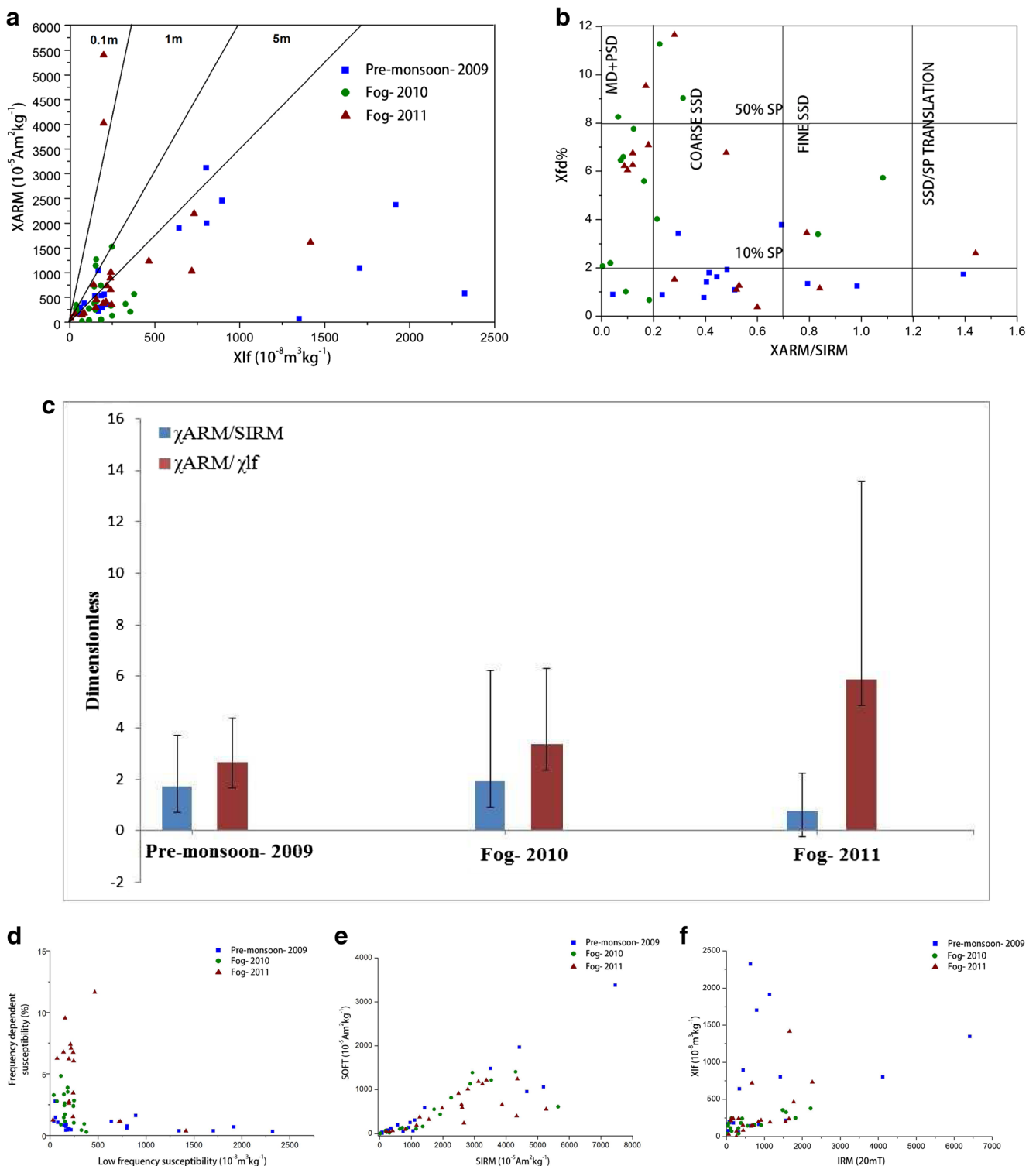


Fig. 3 a–f Relation between different magnetic properties with respect to the observed RDS, where a and b have been modified after King et al. (1982) and Dearing (1999), respectively

more abundant during the fog period. In general, the samples of pre-monsoon period is enriched in finer grain sizes as the dust storms lead to grain size reduction triggered by weathering, abrasion, and attrition of particles, and this promotes transportation and deposition of the particulate matter.

The finer particles are known to be enriched in magnetic minerals which ultimately enhance the magnetism. The coarser particles are more abundant during the fog period because of the effect of humidity and precipitation that prevent dust re-suspension leading to the accumulation of the

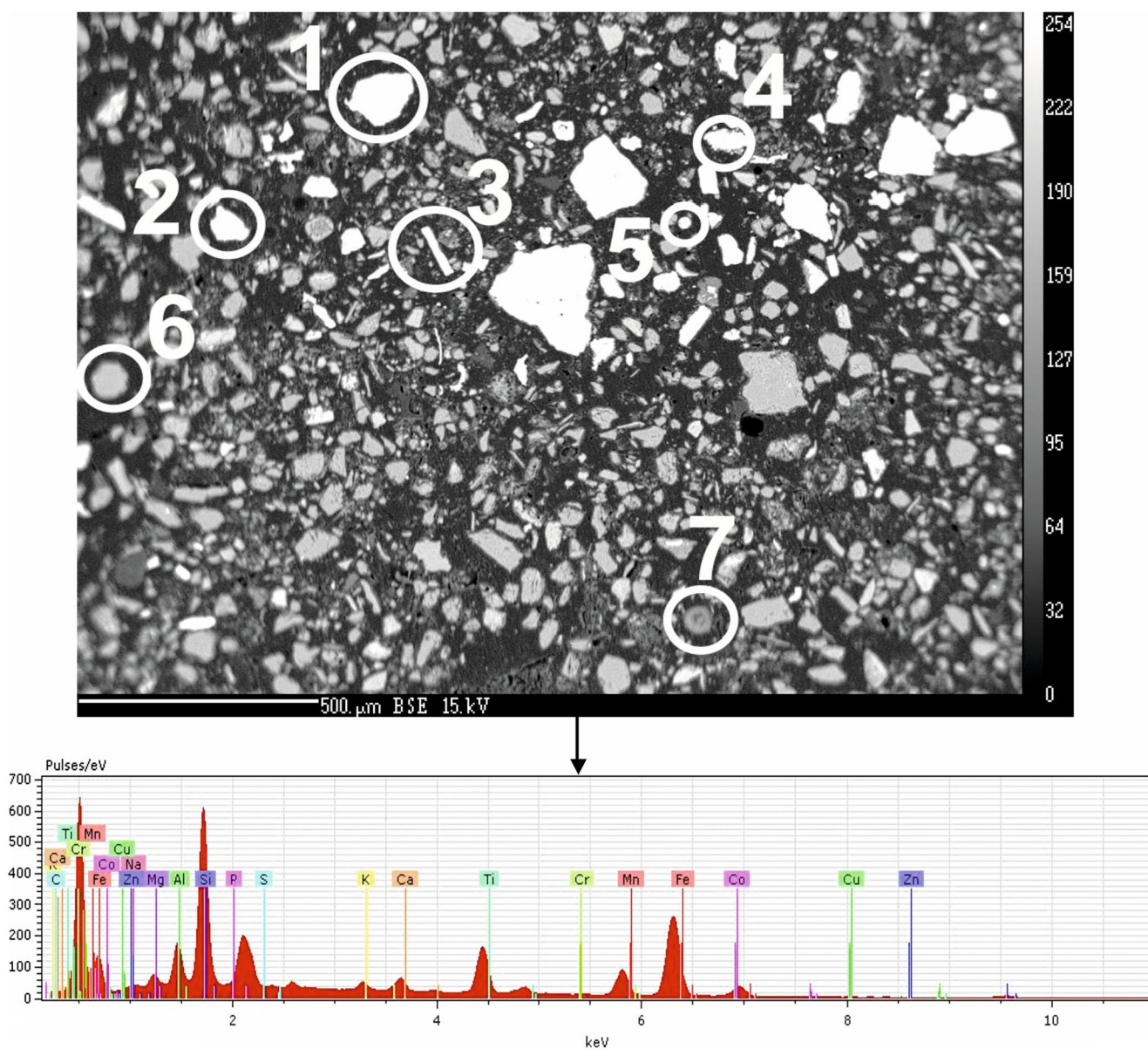


Fig. 4 BSE photomicrographs of RDS showing varied shaped particles (1-subangular, 2-subrounded, 3-acicular, 4-angular, 5-spherule, 6-rounded, and 7-well rounded) with corresponding EDX spectra reflecting elemental abundance and more importantly enrichment of siderophile elements

coarser fraction. The negative correlation between χ_{lf} and $\chi_{fd}\%$ (Fig. 3d) indicates the susceptibility variation resulting from anthropogenic pollution (Canbay et al. 2010). The inverse relationship between susceptibility and $\chi_{fd}\%$ in dust load has been attributed to the contribution of pedogenic SP grains (Sheng-Gao and Shi-Qing 2008). The low $\chi_{fd}\%$ value indicates the presence of coarser magnetic grains (Hay et al. 1997). The susceptibility values of the RDS, observed during the present study, hence, confirm the presence of ferrimagnetic minerals similar to the findings of Wang et al. (2012). The linear correlation between SOFT and SIRM ($R^2 = 0.7$) (Fig. 3e) suggests that the magnetic properties of the RDS are dominated by ferromagnetic minerals (magnetite). Similar observations are reported for the street dust of

China (Peng et al. 2010). In addition, a significant correlation ($R^2 = 0.6$) between χ_{lf} and IRM (measured at 20 mT; Fig. 3f) suggests the predominance of ferrimagnetic minerals in the RDS.

3.2 Morphological and micro-chemical analysis

The morphology of different RDS particles was determined using BSE-SEM aided with energy dispersive spectra (EDS) which provide valuable information about the presence magnetic grains within a sample. About 94–95% of all the particles observed occur as isolated grains and the remaining 3–4% form aggregates. The grains are varied in shape (angular, sub-angular, rounded, well rounded, subrounded, acicular

Fig. 5 X-ray diffraction patterns of two representative RDS from Allahabad city showing the presence of Qtz-Quartz, Or-Orthoclase, Cal-Calcite, Ap-Apatite, Dol-Dolomite, Hem-Hematite, Mag-Magnetite, and Gy-Gypsum

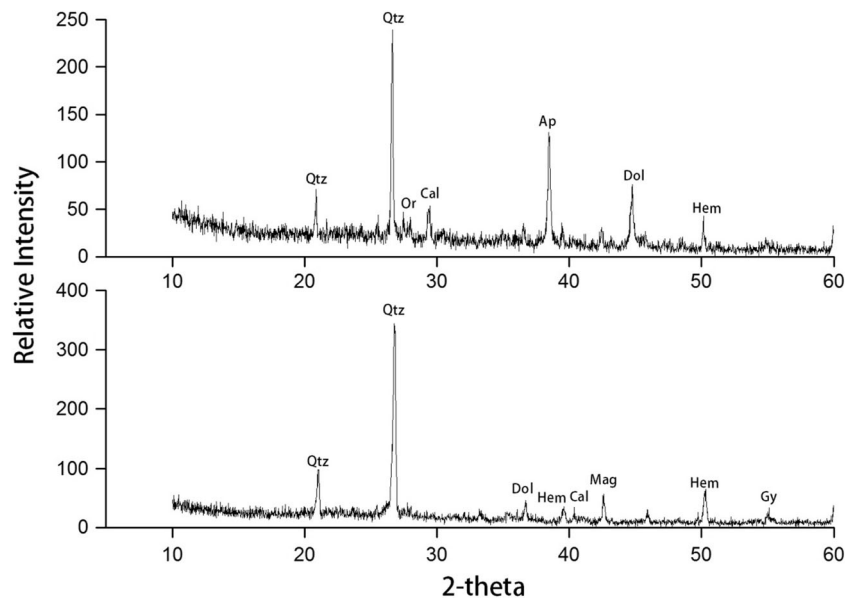


Fig. 6 a Average concentration of major elements, **b** trace elements (including heavy metals) in the RDS with varying seasons where the gray area represents the range of data from present study

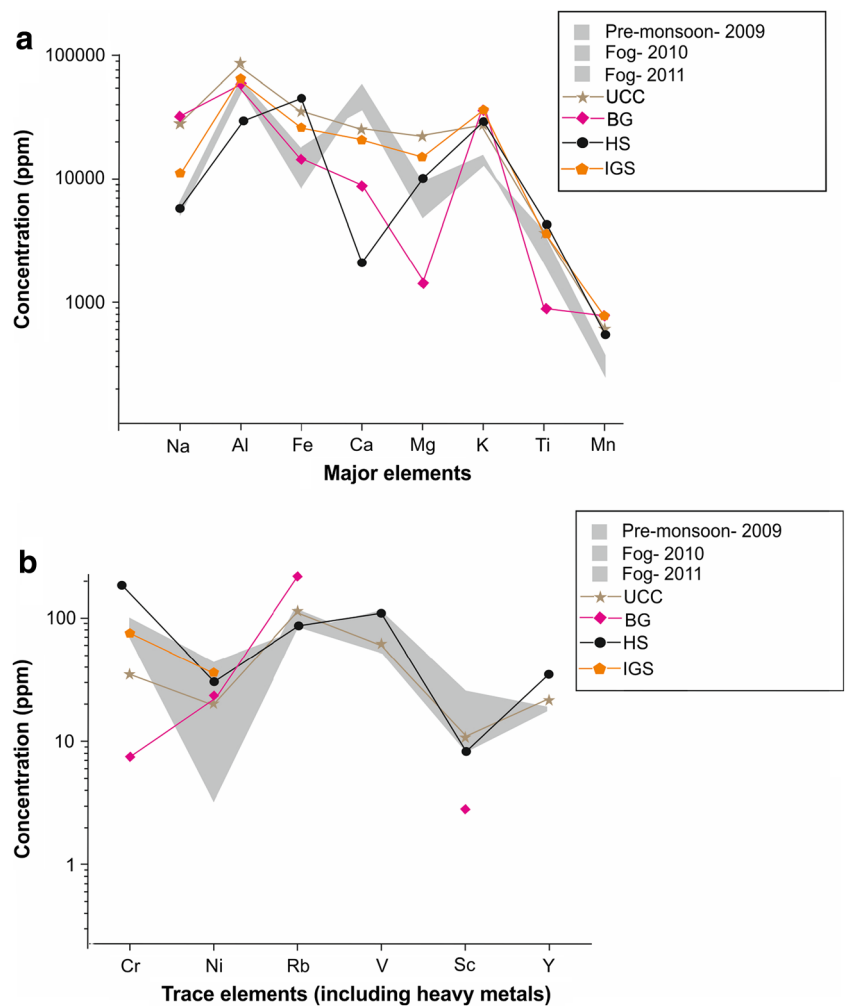


Table 2 Concentration of major and trace elements of RDS during sampling periods

Element	Pre-monsoon-2009 (in ppm)			Fog-2010 (in ppm)			Fog-2011 (in ppm)			UCC ^a (in ppm)	IGS ^b (in ppm)	BG ^c (in ppm)	HS ^d (in ppm)			
	Min.	Max.	Avg.	σ	Min.	Max.	Avg.	σ	Min.					Max.	Avg.	σ
Na	1165	13,539	5508	4210	3153	9258	6133	2317	4021	8465	6015	1801	28,200	11,128	31,974	5787
Mg	446	13,449	4831	5313	1158	12,303	5457	4616	4921	22,906	9314	6780	22,000	15,078	1387	9831
Al	51,512	98,546	63,376	17,571	51,385	59,302	56,099	2712	52,883	62,335	57,794	3176	84,700	64,569	59,170	29,215
K	10,983	15,765	13,222	1694	11,606	18,969	14,977	2366	12,295	17,566	15,412	1837	27,400	35,697	38,104	28,973
Ca	11,957	58,141	37,717	16,790	24,557	90,467	48,078	23,604	38,608	71,599	56,870	12,978	25,000	20,726	8791	2073
Fe	8932	31,817	17,595	10,020	7372	10,520	8558	1192	9498	21,892	13,709	5029	35,000	25,879	14,338	43,435
Mn	271	550	370	133	240	294	267	23	263	503	325	89	600	774	774	542
Ti	1864	9244	3722	2921	1840	2596	2146	319	1649	3165	2294	502	3600	3597	899	4436
Cr	58	127	95	27	47	97	69	20	57	79	67	10	35	75	8	202
Ni	1	167	52	64	3	6	5	1	2	22	10	8	20	36	23	30
Sc	8	51	24	20	3	13	8	4	6	19	11	4	11	N.A.	3	7
V	42	247	109	83	42	62	51	8	36	82	56	15	60	N.A.	N.A.	93
Y	17	18	17	0.2	17	18	18	0.3	17	18	18	0.1	22	N.A.	N.A.	35
Rb	68	67	65	22	90	115	100	10	81	228	125	56	112	N.A.	213	83

N.A. not available

Taylor and McLennan (1985)

Tripathi et al. (2007)

Pati et al., 2008

Bhat and Ghosh, 2001

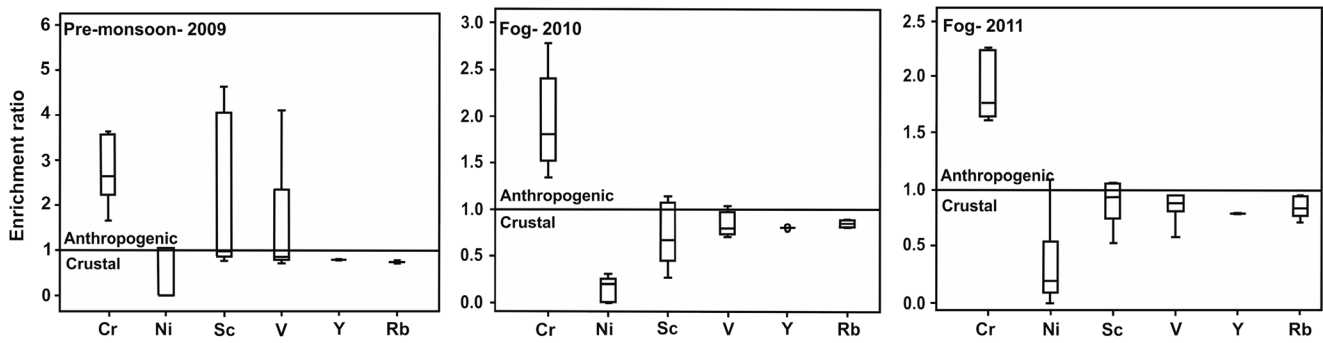


Fig. 7 Enrichment ratio of trace elements (including heavy metals) in RDS of different sampling periods suggesting their derivation mainly from anthropogenic source during pre-monsoon compared to dominant contribution from the crustal source during the fog period

particles; Fig. 4). The spherules observed in the majority of RDS constitute about 1–2% of its bulk volume. The irregular-shaped and brighter particles are anthropogenic in origin derived from vehicular emission or during mechanical wear and tear processes (Goddu et al. 2004). The angular grains range in size from 1 to 180 μm whereas the spherules measure between 10 and 100 μm. The EDS shows the RDS mainly composed of Si, Ti, Fe with Al, Ca, Mn, and other trace elements (Fig. 4). The acicular grains are magnetite, sub-angular grains are quartz, and the platy grains are mainly gypsum. The spherical particles are either Fe-rich or composed of Ca, Al, and Si predominantly (Niyogi et al. 2011).

3.3 X-ray diffraction of RDS

The XRD analysis was used to determine the bulk mineralogy of RDS and to identify the presence of magnetic minerals. The XRD patterns of the RDS are summarized in Fig. 5. About 70–80 vol% of the RDS comprises mineral matter and the remaining constitutes amorphous constituents. The minerals identified include quartz (d: 3.34 Å) with a subordinate amount of orthoclase feldspar (d: 3.29 Å), calcite (d: 3.02 Å), dolomite (d: 2.19 Å), apatite (d: 1.9 Å) possibly derived from both lithogenic and anthropogenic sources while magnetite (d: 1.8 Å) and hematite (d: 3.6 Å) are

Table 3 Principal component analysis carried out for source identification of heavy metals and magnetic properties of three seasons collected from RDS of Allahabad

	Pre-monsoon-2009				Fog-2010				Fog-2011			
	PC1	PC2	PC3	PC4	PC1	PC2	PC3	PC4	PC1	PC2	PC3	PC4
Cr	<i>0.73</i>	<i>0.61</i>	<i>0.29</i>	0.1	0.2	0.07	0.19	<i>0.95</i>	-0.36	-0.12	<i>0.53</i>	-0.52
Ni	<i>0.94</i>	-0.21	-0.13	0.15	0.38	<i>0.64</i>	0.44	<i>0.5</i>	-0.17	<i>0.58</i>	0.22	<i>0.75</i>
Sc	<i>0.92</i>	0.18	<i>0.35</i>	0.06	0.47	<i>0.75</i>	-0.1	0.41	0.03	0.08	<i>0.99</i>	0.03
V	<i>0.62</i>	0.22	<i>0.74</i>	0.08	0.06	0.48	-0.16	<i>0.85</i>	-0.36	0.01	<i>0.93</i>	-0.003
Y	0.1	-0.85	-0.29	0.44	-0.63	-0.34	-0.51	-0.3	-0.82	-0.03	-0.05	0.08
Rb	-0.9	0.07	0.34	-0.22	<i>0.95</i>	0.3	0.09	-0.02	-0.18	<i>0.83</i>	-0.07	<i>0.52</i>
χLF	<i>0.99</i>	0.12	0.06	0.08	<i>0.54</i>	0.34	<i>0.71</i>	0.26	0.13	0.02	<i>0.95</i>	-0.26
FD%	-0.29	-0.05	<i>0.93</i>	-0.1	-0.95	-0.07	-0.01	-0.24	-0.2	0.05	-0.25	<i>0.86</i>
SIRM	<i>0.9</i>	0.29	0.26	0.17	0.37	<i>0.85</i>	0.34	0.19	0.49	-0.73	0.37	0.27
χARM	<i>0.5</i>	0.39	<i>0.74</i>	0.09	-0.01	-0.25	<i>0.97</i>	-0.001	<i>0.97</i>	-0.1	0.03	-0.21
χARM/SIRM	-0.51	-0.82	0.05	-0.21	-0.97	-0.19	-0.1	-0.11	0.52	0.83	-0.11	0.18
SIRM/χLF	-0.06	<i>0.81</i>	0.04	0.45	0.42	<i>0.84</i>	0.15	0.22	0.04	-0.81	-0.54	0.19
χARM/χLF	-0.89	-0.33	0.18	-0.17	-0.73	-0.32	<i>0.59</i>	-0.12	<i>0.84</i>	-0.1	-0.47	-0.24
SOFT	0.94	0.15	0.28	0.1	0.04	<i>0.92</i>	-0.29	0.11	<i>0.84</i>	-0.5	-0.14	0.17
S-ratio%	-0.29	-0.12	-0.04	-0.93	0.01	-0.59	-0.79	-0.03	-0.36	<i>0.82</i>	0.11	0.34
Eigen Values	<i>8.81</i>	<i>2.93</i>	<i>1.75</i>	<i>1.10</i>	<i>8.35</i>	<i>2.85</i>	<i>2.10</i>	<i>1.28</i>	<i>5.62</i>	<i>3.96</i>	<i>2.86</i>	<i>1.60</i>
% of variance	<i>58.74</i>	<i>19.54</i>	<i>11.7</i>	<i>7.37</i>	<i>55.69</i>	<i>19.01</i>	<i>14</i>	<i>8.57</i>	<i>37.48</i>	<i>26.41</i>	<i>19.11</i>	<i>10.7</i>
Cumulative %	<i>58.74</i>	<i>78.28</i>	<i>89.98</i>	<i>97.35</i>	<i>55.69</i>	<i>74.7</i>	<i>88.7</i>	<i>97.27</i>	<i>37.48</i>	<i>63.89</i>	<i>83</i>	<i>93.7</i>

Italic numbers indicate the significant association (>0.5 and <-0.5) of the analyzed principal component

derived from anthropogenic sources. The gypsum (d: 4.27 Å) within the RDS originated in the coal-fired power plant, as the burning of coal generally leads to its formation (Goodarzi 2006). Quartz is the most dominant phase followed by feldspars, oxides (magnetite and hematite), sulfate (gypsum), carbonates (calcite and dolomite), and phosphate (apatite).

3.4 Geochemical analysis

The chemical analysis of the selected major (Na, Mg, Al, K, Ca, Ti, Mn, and Fe) and trace elements (Sc, V, Cr, Ni, Rb, and Y) of the RDS is summarized in Fig. 6a, b and Table 2. The elemental concentrations of the RDS are compared to their possible provenance compositions (Upper Continental Crust (UCC), Taylor and McLennan 1985; Bundelkhand granitoid (BG), Pati et al. 2008; Himalayan sediment (HS), Bhat and Ghosh 2001; Indo-Gangetic sediment (IGS), Tripathi et al. 2007). The UCC, BG, and HS are primarily felsic in nature, whereas the IGS has both argillaceous and marginally carbonaceous constituents. The Ca concentration in the RDS is enriched (37,717 to 56,870 ppm) as compared to the background value (25,000 ppm in UCC, Taylor and McLennan 1985) and K content is also elevated with respect to Na, Mg, Ti, and Mn but depleted compared to reference values of UCC, BG, HS, and IGS. Since Ca and K are ubiquitously observed in all RDS samples worldwide, possibly this observation can be used to differentiate the provenance types (anthropogenic and geogenic) of sediments in a similar setting. The possible cause of Ca enrichment is the presence of modal gypsum derived from the coal-fired captive power plant, Phulpur (zone 5). Misra et al. (2014) earlier suggested that calcite in IGS contributes Ca to the sediments. In contrast, the present study shows that IGS is relatively depleted in Ca and may not be its only source for the Ca enrichment. The Fe concentration is depleted compared to the reference values since the fine powdered fraction (< 74 µm) was analyzed while the coarser fractions were left. However, the presence of ferri- and ferromagnetic minerals in RDS has been verified based on magnetic measurements, BSE-SEM, SEM-EDS, and XRD data. The multicationic pattern of the RDS is similar to the UCC and IGS suggesting its possible derivation from these geogenic sources.

On the other hand, the relatively immobile trace elements (Sc, V, Cr, Ni, Rb, and Y) show variation among the UCC, HS, IGS, and BG (Table 2). The Cr and Ni show inverse relationship negating their possible presence in magnetite in solid solution. The HS and UCC values are showing similar pattern to the RDS but the stated values are low (except Cr and Y) suggesting a dominant anthropogenic contribution rather than crustal load.

3.5 Assessment of metal pollution in RDS

3.5.1 Enrichment ratio

The ER for each element has been calculated on the basis of concentration of measured trace elements in the sample divided by its average concentration in the UCC ($ER = C^{\text{metal/sample}} / C^{\text{metal/UCC}}$). The ER value close to unity suggests the derivation of the metal from crustal sources, while $ER > 1$ indicates its anthropogenic origin (Rajaram et al. 2014; Lin et al. 2016).

The ER for trace elements (Sc, V, Cr, Ni, Rb, and Y) is shown in Fig. 7 for the pre-monsoon-2009, fog-2010, and fog-2011 periods. The higher ER of Sc, V, and Cr in pre-monsoon-2009 samples suggests their possible derivation from metal-alloy industry, vehicular traffic, and coal-fired thermal power plant. The presence of Ni, Rb, and Y suggests their possible derivation from crustal and mixed (traffic and industrial) sources. The $C^{\text{metal}}/C^{\text{UCC}}$ ratio suggests minimal to moderate enrichment of Cr, Sc, and V in RDS compared to ER. Cr is most enriched compared to other metals suggesting its origin from metal-based industries (iron and steel work, heavy engineering, tool making, and metal plating) in the study area.

3.6 Source identification using statistical analyses

The multi-variate statistical analyses of trace elements combined with magnetic characteristics of RDS are helpful to ascertain their possible provenance. The results of the PCA for magnetic parameters and trace element concentration show four principal components with an eigenvalue > 1 extracted for each season (Table 3). The four component dataset explains the cumulative percent total as 97.35% (pre-monsoon-2009), 97.27% (fog-2010), and 93.7% (fog-2011) for the three respective sampling periods. The initial component matrix of the dataset shows that Cr, Ni, Sc, V, and the corresponding magnetic parameters χ_{lf} , SIRM, χ_{ARM} , and SOFT are associated with PC1 for pre-monsoon-2009 which confirms mixed anthropogenic source as a factor originating from industries and traffic with a total 58.74% explained variance. The PC2 shows 19.54% explained variance with a significant SIRM/ χ_{lf} value. V and magnetic parameters ($\chi_{\text{fd}}\%$ and χ_{ARM}) are showing higher values with 11.7% explained variance in PC3 which is related to the crustal origin. During fog-2010, PC1, Rb, and χ_{lf} explain positive loading while Y, $\chi_{\text{fd}}\%$, $\chi_{\text{ARM}}/\text{SIRM}$, $\chi_{\text{ARM}}/\chi_{\text{lf}}$ show negative loading suggesting its crustal input on the RDS (55.69% explained variance). The PC2 in fog-2010 comprised Ni, Sc, SIRM, SIRM/ χ_{lf} , and SOFT as high loading, where Ni and Sc are mainly contributed by both lithogenic and anthropogenic sources with the concentration of magnetic grains, as indicated. The high loading of Cr, Ni, and V during fog-2010 in PC4 suggest its derivation from traffic and industrial sources. In fog-2011, Ni, Rb, $\chi_{\text{ARM}}/\text{SIRM}$, and S-ratio show positive loading in PC2

with the presence of magnetite and hematite in finer grains while SIRM with negative loading depicts the origin from both lithogenic and anthropogenic processes. PC3 loading in fog-2011 includes Cr, Sc, V, and χ_{lf} suggesting its anthropogenic input from vehicular activities and industries.

4 Conclusions

Magnetic measurements unequivocally demonstrate the variable enrichment of heavy metals (Avg. Σ : 224.11 to 362.66 ppm) in the RDS of Allahabad city belonging to pre-monsoon-2009, fog-2010 and 2011 periods. The industrial areas (Naini and Phulpur; zone 5) have maximum heavy metal content (Avg. Σ : 206.95 to 544.98 ppm), which is also reflected in the elevated magnetic susceptibility values for the three sampling periods. The pollution load diminishes in the following order: zones 5, 3, 4, 2, and 1, independent of seasonal variations. The cumulative susceptibility value varies from 39.46 to $2302.96 \times 10^{-8} \text{ m}^3 \text{ kg}^{-1}$ during the pre-monsoon-2009 period. In contrast, the lowering of cumulative susceptibility values is observed in the RDS belonging to fog-2010 (37.87 to $379.2 \times 10^{-8} \text{ m}^3 \text{ kg}^{-1}$) and fog-2011 (29.42 to $1415.88 \times 10^{-8} \text{ m}^3 \text{ kg}^{-1}$). It is interesting to observe about a three-fold increase in the cumulative susceptibility values of RDS of pre-monsoon-2009 period compared to that of fog-2010 and a two-fold increase with reference to fog-2011 samples. The study also shows that the magnetic grains are mainly PSD, MD, and coarse SSD having both ferro- and ferrimagnetic grains. This suggests that both finer ($< 1 \mu\text{m}$) as well as coarser ($> 10 \mu\text{m}$) magnetic grains are present in the RDS. The particles of varied shapes (mainly angular-subangular) and sizes (~ 1 – $180 \mu\text{m}$) observed in the BSE-SEM images indicate a very poor sorting of the RDS and confirms their derivation from proximal lithogenic and anthropogenic sources. The nature of magnetic minerals, their abundance, and the size-range observed on the basis of magnetic measurements are also supported by XRD and BSE-SEM data.

The average major elemental concentration patterns of the RDS show similarity to the proposed proximal and distal geogenic source domains (UCC and IGS). Ca, one of the major elements in the RDS, is elevated more than 10 times compared to its concentration in geogenic sources. The presence of gypsum (Ca: 23.3 wt.%), calcite (Ca: 40.04 wt.%), and dolomite (Ca: 21.73 wt.%) in RDS, identified by BSE-SEM study and XRD patterns, is consistent with the observed anomalous Ca increase (3.77–5.69 wt.%). This strongly supports the derivation of Ca from anthropogenic and geogenic sources. The trace elements (Sc, V, Cr, Ni, Rb, and Y) are elevated in pre-monsoon samples compared to those belonging to fog-2010 and 2011. The provenance of the sediment load comprises felsic igneous rocks (BG) and arenaceous-argillaceous sedimentary rocks (HS and IGS) that are depleted

in siderophile elements, and hence, the elevated Cr and variable Ni and V contents strongly advocate their derivation from anthropogenic as well as industrial sources.

The ER of heavy metals in RDS further lends credence to the inferences obtained from magnetic measurements. The present study suggests that the sediments are derived from multiple sources with a dominance of anthropogenic load. This further reaffirms the applicability of magnetic measurements as a simple, rapid, and cost-effective technique to evaluate pollution load in local and regional scales and also for tracing the provenance of the dust load effectively.

Acknowledgements AN acknowledges the University of Allahabad for UGC-CRET Fellowship during the study. This study forms a part of the D.Phil. thesis of AN. JKP thanks PLANEX, Department of Space, Government of India and GRBMP, Ministry of Environment and Forest, Government of India for their financial support. The authors sincerely acknowledge and thank the two anonymous reviewers for their thorough review, excellent comments, and suggestions. The help and suggestions from the Editor-in-Chief are greatly appreciated.

References

- Adachi K, Tainosho Y (2005) Single particle characterization of size-fractionated road sediments. *Appl Geochem* 20(5):849–859. <https://doi.org/10.1016/j.apgeochem.2005.01.005>
- Bhat MI, Ghosh SK (2001) Geochemistry of the 2.51 Ga old Rampur group pelites, western Himalayas: implications for their provenance and weathering. *Precambrian Res* 108(1-2):1–16. [https://doi.org/10.1016/S0301-9268\(00\)00139-X](https://doi.org/10.1016/S0301-9268(00)00139-X)
- Bian Y, Ouyang T, Zhu Z, Huang N, Wan H, Li M (2014) Magnetic properties of agricultural soil in the Pearl River Delta, South China—spatial distribution and influencing factor analysis. *J Appl Geophys* 107:36–44. <https://doi.org/10.1016/j.jappgeo.2014.05.003>
- Bourliva A, Papadopoulou L, Aidona E (2016) Study of road dust magnetic phases as the main carrier of potentially harmful trace elements. *Sci Total Environ* 553:380–391. <https://doi.org/10.1016/j.scitotenv.2016.02.149>
- Canbay M, Aydin A, Kurtulus C (2010) Magnetic susceptibility and heavy-metal contamination in topsoils along the Izmit gulf coastal area and Izaytas (Turkey). *J Appl Geophys* 70(1):46–57. <https://doi.org/10.1016/j.jappgeo.2009.11.002>
- Chakarvorty M, Pati JK, Patil SK, Shukla S, Niyogi A, Sharaf AK (2014) Physical characterization, magnetic measurements, REE geochemistry and bio-monitoring of dust-load accumulated during a protracted winter fog period and their implications. *Environ Monit Assess* 186(5):2965–2978. <https://doi.org/10.1007/s10661-013-3594-4>
- Dearing JA (1999) Susceptibility. In: Walden J, Oldfield F, Smith JP (eds) *Environmental magnetism: a practical guide*. Quaternary research association, Cambridge, pp 35–62
- Dekkers MJ (1997) *Environmental magnetism: an introduction*. *Neth J Geosci* 76(1/2):163–182. <https://doi.org/10.1023/A:1003122305503>
- Evans ME, Hellers F (2003) *Environmental magnetism principles and applications of enviromagnetics*. Academic Press, USA, pp 1–295
- Fedotov PS, Ermolin MS, Karandashev VK, Ladonin DV (2014) Characterization of size, morphology and elemental composition of nano-, submicron, and micron particles of street dust separated

- using field- flow fractionation in a rotating coiled column. *Talanta* 130:1–7. <https://doi.org/10.1016/j.talanta.2014.06.040>
- Goddu SR, Appel E, Jordanova D, Wehland F (2004) Magnetic properties of road dust from Visakhapatnam (India)—relationship to industrial pollution and road traffic. *Phys Chem Earth* 29(13–14):985–995. <https://doi.org/10.1016/j.pce.2004.02.002>
- Goodarzi F (2006) Characteristics and composition of fly ash from Canadian coal-fired power plants. *Fuel* 85(10–11):1418–1427. <https://doi.org/10.1016/j.fuel.2005.11.022>
- Hay KL, Dearing JA, Baban SMJ, Loveland P (1997) A preliminary attempt to identify atmospherically-derived pollution particles in English topsoils from magnetic susceptibility measurements. *Phys Chem Earth* 22(1–2):207–210. [https://doi.org/10.1016/S0079-1946\(97\)00104-3](https://doi.org/10.1016/S0079-1946(97)00104-3)
- Jones S, Richardson N, Bennett M, Hoon SR (2015) The application of magnetic measurements for the characterization of atmospheric particulate pollution within the airport environment. *Sci Total Environ* 502:385–390. <https://doi.org/10.1016/j.scitotenv.2014.09.010>
- Jordanova D, Jordanova N, Petrov P (2015) Magnetic susceptibility of road deposited sediments at a national scale—relation to population size and urban pollution. *Environ Pollut* 189:239–251
- Karimi R, Ayoubi S, Jalalian A, Sheikh-Hosseini AR, Afyuni M (2011) Relationship between magnetic susceptibility and heavy metals in urban topsoils in the arid region of Isfahan, central Iran. *J Appl Geophys* 74(1):1–7. <https://doi.org/10.1016/j.jappgeo.2011.02.009>
- King J, Banerjee SK, Marvin J, Özdemir Ö (1982) A comparison of different magnetic methods for determining the relative grain-size of magnetite in natural materials—some results from lake-sediments. *Earth Planet Sc Lett* 59(2):404–419. [https://doi.org/10.1016/0012-821X\(82\)90142-X](https://doi.org/10.1016/0012-821X(82)90142-X)
- Li R, Cai G, Wang J, Ouyang W, Cheng H, Lin C (2014) Contents and chemical forms of heavy metals in school and roadside topsoils and road-surface dust of Beijing. *J Soils Sediments* 14(11):1806–1817. <https://doi.org/10.1007/s11368-014-0943-z>
- Lin M, Gui H, Wang Y, Peng W (2016) Pollution characteristics, source apportionment, and health risk of heavy metals in street dust of Suzhou, China. *Environ Sci Pollut Res* 24(2):1987–1998. <https://doi.org/10.1007/s11356-016-7934-0>
- Lu SG, Bai SQ, Xue QF (2007) Magnetic properties as indicators of heavy metals pollution in urban topsoils: a case study from the city of Luoyang, China. *Geophys J Int* 171(2):568–580. <https://doi.org/10.1111/j.1365-246X.2007.03545.x>
- Maher BA (1998) Magnetic properties of modern soils and quaternary loessic paleosols: paleoclimatic implications. *Palaeogeogr Palaeoclimatol Palaeoecol* 137(1–2):25–54. [https://doi.org/10.1016/S0031-0182\(97\)00103-X](https://doi.org/10.1016/S0031-0182(97)00103-X)
- Maher BA (2011) The magnetic properties of quaternary aeolian dusts and sediments, and their palaeoclimatic significance. *Aeolian Res* 3(2):87–144. <https://doi.org/10.1016/j.aeolia.2011.01.005>
- Meena NK, Maiti S, Shrivastava A (2011) Discrimination between anthropogenic (pollution) and lithogenic magnetic fraction in urban soils (Delhi, India) using environmental magnetism. *J Appl Geophys* 73:121–129
- Misra A, Gaur A, Bhattu D, Ghosh S, Dwivedi AK, Dalai R, Paul D, Gupta T, Tare V, Mishra SK, Singh S, Tripathi SN (2014) An overview of the physico-chemical characteristics of dust at Kanpur in the central Indo-Gangetic basin. *Atmos Environ* 97:386–396. <https://doi.org/10.1016/j.atmosenv.2014.08.043>
- Niyogi A, Pati JK, Patel SC, Panda D, Patil SK (2011) Anthropogenic and impact spherules: morphological similarity and chemical distinction— a case study from India and its implications. *J Earth Syst Sci* 120(6):1043–1054. <https://doi.org/10.1007/s12040-011-0125-y>
- Pandey M, Pandey AK, Mishra A, Tripathi BD (2017) Speciation of carcinogenic and non-carcinogenic metals in respirable suspended particulate matter (PM₁₀) in Varanasi, India. *Urban Climate* 19:141–154. <https://doi.org/10.1016/j.uclim.2017.01.004>
- Pant P, Baker SJ, Shukla A, Maikawa C, Godri Pollitt KJ, Harrison RM (2015) The PM₁₀ fraction of road dust in the UK and India: characterization, source profiles and oxidative potential. *Sci Total Environ* 530–531:445–452
- Pati JK, Reimold WU, Koeberl C, Pati P (2008) The Dhala structure, Bundelkhand craton, Central India—eroded remnant of a large Paleoproterozoic impact structure. *Meteorit Planet Sci* 43(8):1383–1398. <https://doi.org/10.1111/j.1945-5100.2008.tb00704.x>
- Peng L, Xiao-Ke I Q, Xin-Wen X, Xu-Bin L, Yu-Fang S (2010) Magnetic properties of street dust: a case in Xi'an city, Shaanxi province, China. *Chinese J Geophys Ch* 53(1):113–120
- Pipal AS, Kulshrestha A, Taneja A (2011) Characterization and morphological analysis of airborne PM_{2.5} and PM₁₀ in Agra located in north central India. *Atmos Environ* 45:3621–3630
- Qiao Q, Zhang C, Huang B, Piper JDA (2011) Evaluating the environmental quality impact of the 2008 Beijing Olympic games: magnetic monitoring of street dust in Beijing Olympic park. *Geophys J Int* 187(3):1222–1236. <https://doi.org/10.1111/j.1365-246X.2011.05195.x>
- Rai P, Chakraborty A, Mandariya AK, Gupta T (2016) Composition and source apportionment of PM₁₀ at urban site Kanpur in India using PMF coupled with CBPF. *Atmos Res* 178–179:506–520
- Rajaram BS, Suryawanshi PV, Bhanarkar AD, Rao CVC (2014) Heavy metals contamination in road dust in Delhi city, India. *Environ Earth Sci* 72(10):3929–3938. <https://doi.org/10.1007/s12665-014-3281-y>
- Robertson DJ, Taylor KG, Hoon SR (2003) Geochemical and mineral magnetic characterisation of urban sediment particulates, Manchester, UK. *Appl Geochem* 18(2):269–282. [https://doi.org/10.1016/S0883-2927\(02\)00125-7](https://doi.org/10.1016/S0883-2927(02)00125-7)
- Sagnotti L, Macrì P, Egli R, Mondino M (2006) Magnetic properties of atmospheric particulate matter from automatic air sampler stations in Latium (Italy): toward a definition of magnetic fingerprints for natural and anthropogenic PM₁₀ sources. *J Geophys Res* 111(B12):1–17. <https://doi.org/10.1029/2006JB004508>
- Sheng-Gao L, Shi-Qing B (2008) Magnetic characterization and magnetic mineralogy of the Hangzhou urban soils and its environmental implications. *Chinese J Geophys Ch* 51(3):549–557
- Szuskiewicz M, Magiera T, Kapička A, Petrovský E, Grison H, Gołuchowska B (2015) Magnetic characteristics of industrial dust from different sources of emission: a case study of Poland. *J Appl Geophys* 116:84–92. <https://doi.org/10.1016/j.jappgeo.2015.02.027>
- Taylor SR, McLennan SM (1985) The continental crust; its composition and evolution; an examination of the geochemical record preserved in sedimentary rocks. Blackwell, Oxford, p 312
- Tripathi JK, Ghazanfari P, Rajamani V, Tandon SK (2007) Geochemistry of sediments of the Ganges alluvial plains: evidence of large-scale sediment recycling. *Quatern Int* 159(1):119–130. <https://doi.org/10.1016/j.quaint.2006.08.016>
- Wang XS, Qin Y (2005) Correlation between magnetic susceptibility and heavy metals in urban topsoil: a case study from the city of Xuzhou, China. *Environ Geol* 49(1):10–18. <https://doi.org/10.1007/s00254-005-0015-1>
- Wang G, Xia DS, Liu XM, Chen FH, Yu Y, Yang LP, Chen JH, Zhou AF (2008) Spatial and temporal variation in magnetic properties of street dust in Lanzhou City, China. *Sci Bull* 53(12):1913–1923
- Wang G, Oldfield F, Xia D, Chen F, Liu X, Zhang W (2012) Magnetic properties and correlation with heavy metals in urban street dust: a case study from the city of Lanzhou, China. *Atmos Environ* 46:289–298
- Wang XS (2016) Investigation of the pollution in the street dust at Xuzhou, China, using magnetic, micro-morphological and Mössbauer spectra analyses. *Environ Earth Sci* 75(10):899. <https://doi.org/10.1007/s12665-016-5731-1>
- WHO Global Urban Ambient Air Pollution Database (update 2016) (<http://www.thehindu.com/news/cities/Delhi/delhi-is-not-the-most>

- polluted-city-in-the-world-who/article8589775.ece, accessed on 09–11-2016)
- Yang T, Liu Q, Li H, Zeng Q, Chan L (2010) Anthropogenic magnetic particles and heavy metals in the road dust: magnetic identification and its implications. *Atmos Environ* 44(9):1175–1185
- Zhang M, Lu X, Chen H, Gao P, Fu Y (2015) Multi-element characterization and source identification of trace metal in road dust from an industrial city in semi-humid area of Northwest China. *J Radioanal Nucl Chem* 303(1):637–646. <https://doi.org/10.1007/s10967-014-3300-1>